IEEE Photonics Journal
An IEEE Photonics Society Publication

Open Access

Miniature Reflection-Type Optical Displacement Sensor Incorporating a Projected Beam

Volume 7, Number 1, February 2015

Yong-Geon Lee
Hak-Soon Lee
Sang-Shin Lee

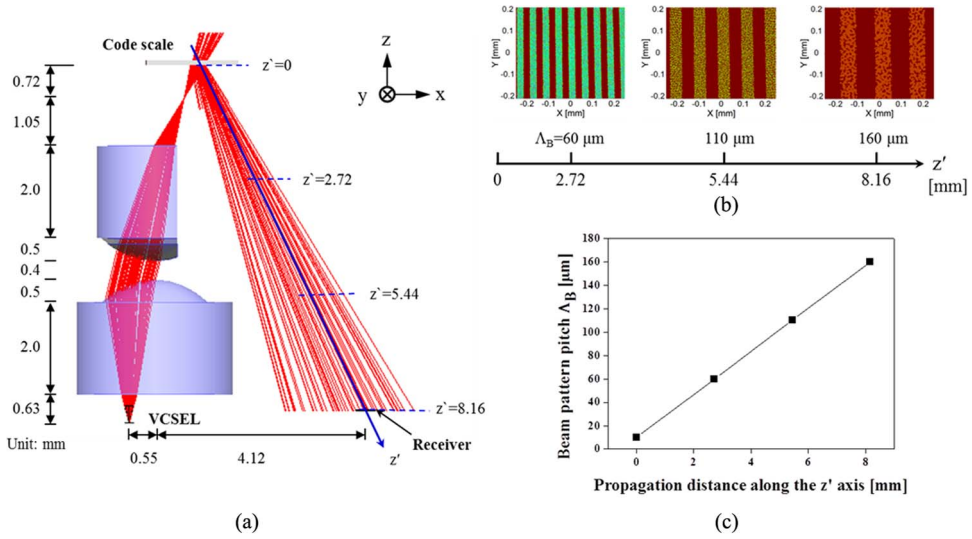

DOI: 10.1109/JPHOT.2014.2387261
1943-0655

Miniature Reflection-Type Optical Displacement Sensor Incorporating a Projected Beam

Yong-Geon Lee, Hak-Soon Lee, and Sang-Shin Lee

Department of Electronic Engineering, Kwangwoon University, Seoul 139-701, Korea

DOI: 10.1109/JPHOT.2014.2387261

Manuscript received October 25, 2014; accepted December 13, 2014. Date of publication January 1, 2015; date of current version January 20, 2015. This work was supported in part by the National Research Foundation of Korea (NRF) under Grant 2013-008672, funded by the Korean government (MSIP), and in part by a research grant from Kwangwoon University in 2014. Corresponding author: S.-S. Lee (e-mail: slee@kw.ac.kr).

Abstract: We embody a miniature reflection-type optical displacement sensor tapping into a projected beam that features high structural tolerance. A code scale with periodic patterns spatially encrypts the projected beam, which is established by imaging a collimated beam from a vertical-cavity surface-emitting laser via an aspheric lens, and linearly expands it, so as to be decoded by a receiver that comprises four serially cascaded identical photodetector cells. For the modulated beam, we observe a pitch increase with a rate of 18 μm/mm along the propagation direction. The two quadrature signals Sig-A and Sig-B derived from the PD signals exhibit a 90° phase relationship. The proposed sensor has been designed via ray-optic simulations and embodied through passive alignment, combined with plastic injection mold. We achieve a positional resolution of $\sim$10 μm from either of Sig-A and Sig-B. By concurrently considering the two quadrature outputs, we efficiently enhance the resolution to 2.5 μm, with the discovered direction of displacement. Finally, we thoroughly investigate the crucial dependence of the sensor performance on the positional tolerance pertaining to the constituent elements, which is discovered to be as large as $+/-$ 100 μm, under a certain resolution.

Index Terms: Sensors, micro-optics, electro-optical systems, gratings.

1. Introduction

An encoder is widely perceived as an indispensable displacement/position sensing tool for a variety of applications, including robotic manipulators for automatic systems, consumer electronics gadgets, medical equipment, printers, cameras, motion sensing systems, and biosensors [1]–[9]. In particular, an optical version of the displacement sensor offers advantages in terms of its high sensitivity, light weight, and imperviousness to ubiquitous electromagnetic interference. The photonic sensor, which involves a code scale, a light source, a receiver based on photodetectors (PDs), and a signal processing circuit, is preferably required to satisfy compact size and low cost [1], [2], [10]–[12]. Depending on the arrangement of the constituent components, the sensor is classified into reflection [1]–[7] or transmission [13]–[17] types. Previously, compact reflection-type sensors resorting to an index grating structure in combination with a beam shaper were reported, drawing upon a collimated beam [4]. To obtain a resolution that is equivalent to the pitch of the code scale, and discern the direction of displacement, most of the constituent components,

including the index grating and the receiver consisting of extremely small PDs, should be delicately controlled in terms of their position and dimension [2]–[6]. It should be stated that in order to boost the resolution by reducing the pitch of the code scale, the pitch of the index grating or the PD cells themselves need to diminish accordingly, due to the use of collimated beam optics. We have recently reported on a displacement sensor that adopts a collimated beam. The beam emanates from either a single-mode or a multimode vertical-cavity surface-emitting laser (VCSEL), and it converges exactly on the code scale so as to be encrypted [5]. The sensor only offers a single output from one piece of the PD, without discerning the direction of the displacement, while the realized positional resolution is merely comparable to the pitch of the code scale grating. Hence, a projected beam instead of a collimated beam needs to be principally considered, in order to substantially alleviate the unavoidable stringent restrictions imposed on the sophisticated tailoring of the receiver or the index grating, originating from a reduction in the code scale pitch. In this paper, we demonstrate a miniature optical displacement sensor that takes advantage of a projected beam encoded by a rotary code scale incorporating a reflection grating. We adopt a receiver that is comprised of four serially concatenated PD cells, in order to analyze the incident spatially modulated projected beam. The proposed sensor is meticulously designed by using ray-optic-based simulations, and it is manufactured through a passive alignment scheme in conjunction with a plastic injection molding technique. Both of the quadrature signals that originate from the receiver are simultaneously taken into account, and we can effectively achieve a resolution that is equivalent to one quarter of the pitch of the code scale, with the discerned direction of the displacement. Finally, we have rigorously inspected the dependence of the sensor performance on the positional alignment of the constituent components, thereby validating the high structural tolerance.

2. Proposed Highly Tolerant Displacement Sensor Based on a Projected Beam and Its Design

The proposed compact optical displacement sensor consists of an optical head in tandem with a rotary code scale, as illustrated in Fig. 1(a). For the optical head, a light beam emanating from a VCSEL is collimated by the first aspheric lens, and subsequently projected by the second aspheric lens. The projected beam is selectively reflected by a grating with a pitch of Λ_C that is engraved on the code scale, propagating in the form of a spatially modulated pattern of pitch Λ_B, which progressively increases. The encoded beam is ultimately accepted and analyzed by a receiver employing four serially concatenated identical PD cells, denoted PD1 through PD4. As implied in Fig. 1(a), the projected beam initially starts from the site of the code scale, assuming a periodic pattern with a pitch of $\Lambda_B = \Lambda_C$. The beam gradually expands along the central z'-direction, so that the pattern pitch is presumed to increase with the propagation distance in a linear fashion. The receiver is designed in such a way that the width of each of the four PD cells is, in principle, in charge of one quarter of the enlarged pitch of the corresponding projected beam. We believe the proposed optical sensor to be highly recommendable in terms of its flexible design, due to the fact that the pattern pitch of the projected beam may be adaptively adjusted in accordance with the size of the receiver. As sketched in Fig. 1(b), we attempt to elucidate the operation of the displacement sensor by referring to various sensor signals of concern. The light powers impinging upon the PD cells belonging to the receiver periodically oscillate between a maximum and minimum level, depending on the displacement of the code scale, giving rise to the corresponding PD signals, such as PS1 through PS4. The sinusoidal-like signals stemming from two adjacent PD cells are meant to exhibit a phase difference of 90°. Those original PD signals adequately experience a signal processing, where PS1 and PS3 are compared to each other to lead to one sensor output of Sig-A, while PS2 and PS4 are similarly processed to result in the other output of Sig-B. As implied in Fig. 1(b), Sig-A and B establish a pair of quadrature signals with a phase relationship of $\phi = 90°$. The sign of ϕ hinges on the direction of the displacement of the code scale, while the pitch of the incoming projected beam determines its magnitude, relative to the dimension of the PD cells. As a consequence, by separately

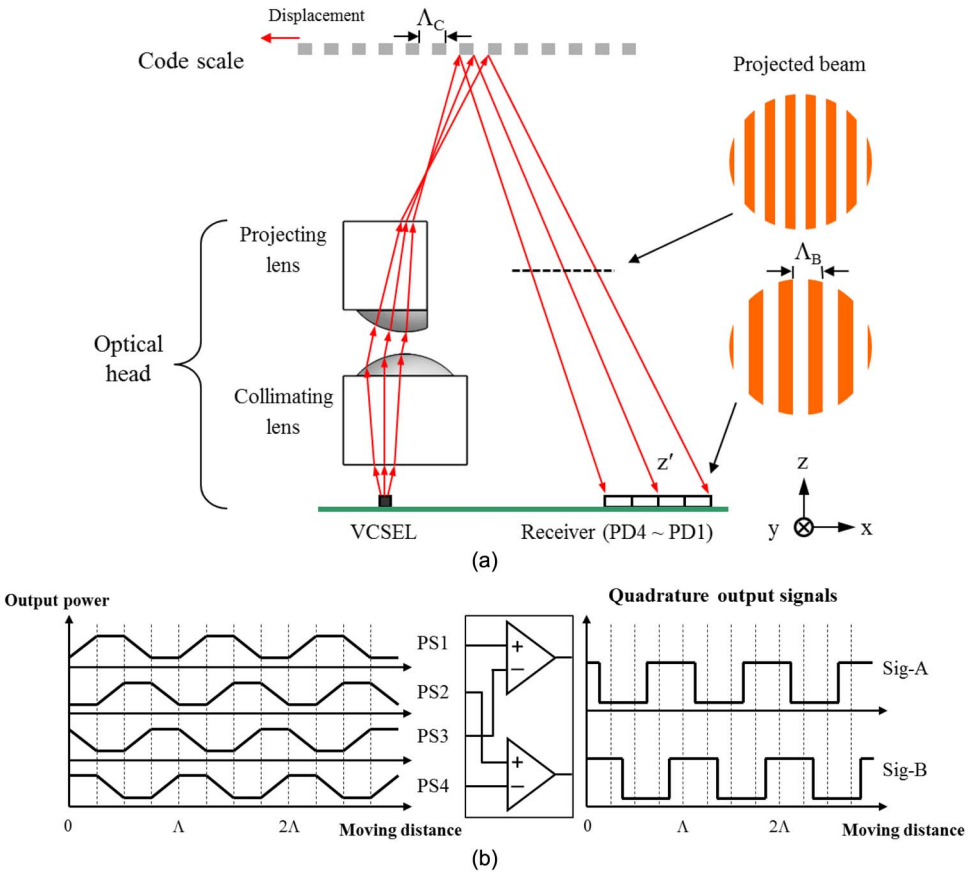

Fig. 1. Proposed optical displacement sensor incorporating a projected beam. (a) Configuration and (b) four PD signals from the receiver, which are signal processed to provide two quadrature pulse signals.

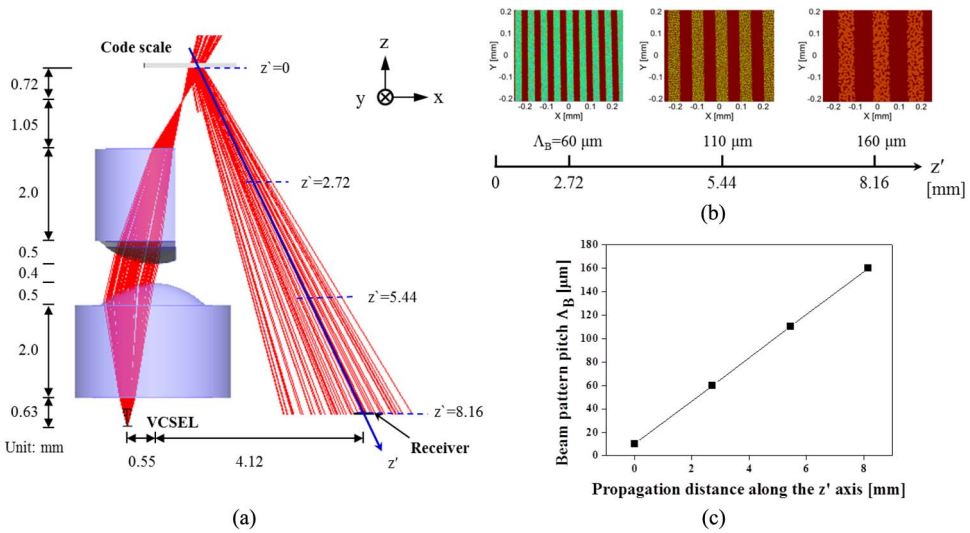

Fig. 2. (a) Designed displacement sensor with the beam trajectory manifested. (b) Pattern profile of the projected beam. (c) Pitch of the beam pattern with the propagation distance.

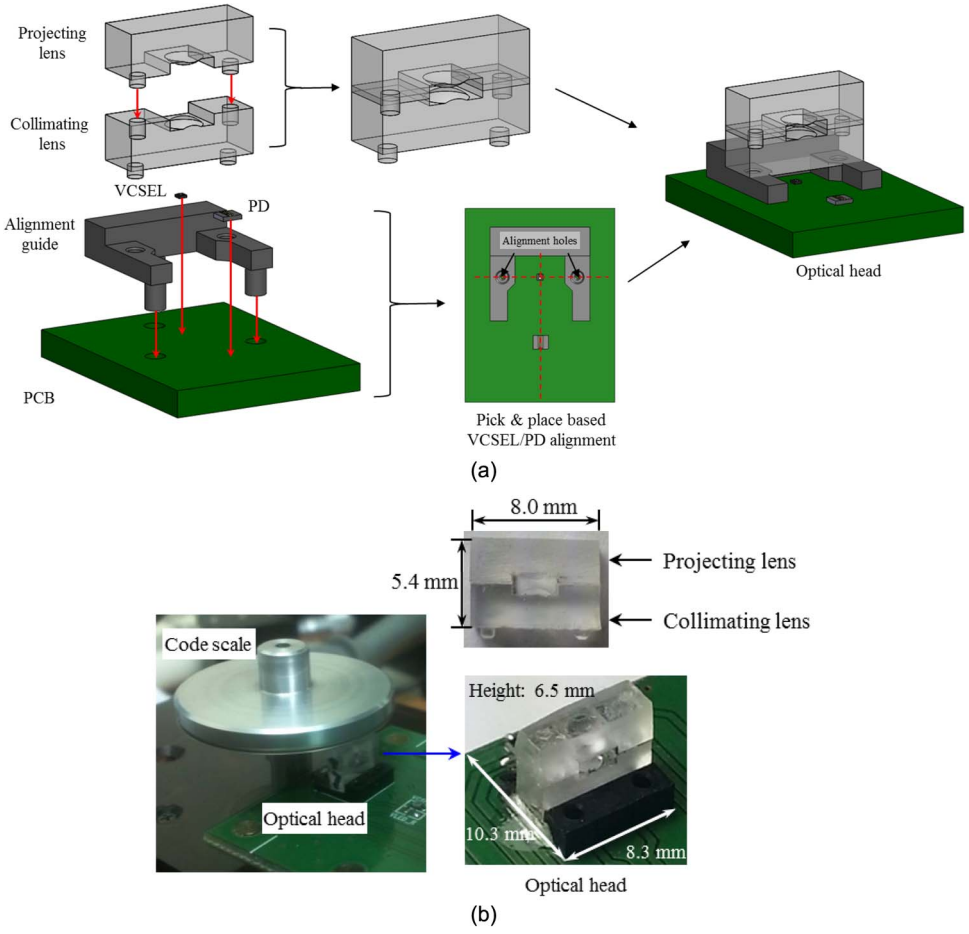

Fig. 3. (a) Construction of the optical displacement sensor via passive assembly mediated by an alignment guide. (b) Completed optical displacement sensor.

dealing with the quadrature signals (either Sig-A or Sig-B), we can simply succeed in measuring the magnitude of displacement initiated by the code scale with a resolution equivalent to its pitch Λ_C. If both Sig-A and B are concurrently taken into account, the direction of the displacement is readily disclosed. Moreover, the resolution can be effectively improved by a factor of four, to become as good as $\Lambda_C/4$.

We have designed and assessed our displacement sensor, by thoroughly carrying out simulations assisted by a ray-optic tool, LightTools. As shown in Fig. 2(a), we use a single-mode VCSEL at $\lambda = 850$ nm with a divergence of 30° for the light source, while the receiver, with a width of 160 μm, uses four identical PD cells, each of 40 μm. A combination of two aspheric lenses in polycarbonate $(n = 1.568)$ is exploited to collimate and project the beam emerging from the VCSEL. The collimating lens is designed to have structural parameters of 2.60-mm diameter, 1.48-mm radius, -2.66×10^{-1} conic constant, and 4th, 6th, and 8th coefficients of -8.28×10^{-3}, -2.57×10^{-3}, and -1.05×10^{-3}, respectively. The projecting lens has the same parameters as the collimating lens, except for the different diameter of 3.40 mm. A rotary code scale of 13.5-mm radius, used for inducing displacement, is modeled as a reflection grating with a 10-μm pitch. In an effort to facilitate the reception of the beam emitted by the VCSEL by the receiver, the collimating lens is positioned 0.55 and 0.63 mm away from the VCSEL along the x- and z-axes, respectively. The projecting lens is vertically separated from the collimating lens by 0.4 mm, so that the incident collimated beam focuses 1.05 mm before the code scale. The interval between the code scale and the projecting lens is determined to be 1.77 mm. Hence, the

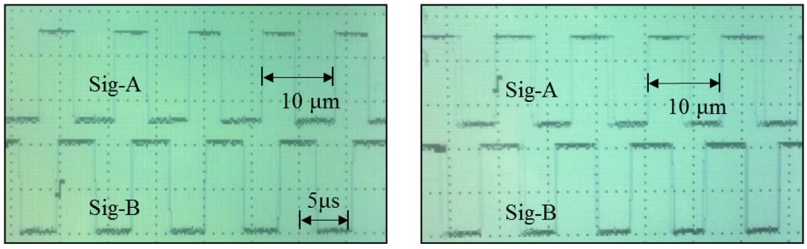

Fig. 4. Measured sensor output signals of Sig-A and Sig-B for (a) clockwise and (b) counter-clockwise directions.

pattern pitch of the projected beam becomes approximately $\Lambda_B = 160$ μm at the site of the receiver, as desired. The PD receiver is horizontally offset from the VCSEL by 4.67 mm. In a bid to scrutinize the characteristics of the projected beam for the designed optical sensor, we denote the direction along the center of the projected beam as the z′-axis, passing through the center of the PD analyzer. The locations of the code scale and the PD receiver correspond to $z' = 0$ and 8.16 mm, respectively. We monitor the profile of the travelling projected beam and its pattern pitch at several locations. As plotted in Fig. 2(b), the projected beam linearly expands with the propagation distance, as expected. As plotted in Fig. 2(c), the pitch starts from $\Lambda_B = 10$ μm at $z' = 0$, evolving to 60 and 110 μm at $z' = 2.72$ and 5.44 mm, respectively. The pitch ultimately reaches $\Lambda_B = 160$ μm, at the position of the PD receiver. As a result, the pitch turns out to increase along the propagation direction at a rate of 18 μm/mm. Next, as addressed in Fig. 1(b), we have theoretically confirmed for the designed sensor the generation of the two pulse signals of Sig-A and B, alongside four sinusoidal-like signals available from the receiver, like PS1 through PS4. As predicted, PS1- all assume a period of 10 μm. In regard to Sig-A and B, the pitch is similarly 10 μm, while a positive or negative 90° phase relationship is acquired, subject to the direction of the displacement of the code scale.

3. Construction of the Proposed Displacement Sensor and Its Characterization

Fig. 3(a) briefly describes the procedure for manufacturing the designed optical sensor. The optical head has been passively created through a cost-effective pick-and-place scheme, where with reference to an alignment guide, a single-mode 850-nm VCSEL source from Oclaro was precisely aligned with four PD cells, each 40 μm wide, via both collimating and projecting lenses linked to a code scale. As displayed in Fig. 3(b), the optical head, with dimensions of 10.3 (W) $\times$ 8.3 (L) $\times$ 6.5 (H) mm^3, appears to encompass collimating and projecting aspheric lenses that are produced by means of plastic injection molding in polycarbonate. We completed the displacement sensor by precisely matching the optical head with a rotary code scale integrated with a grating of 10-μm pitch, which engages alternating highly reflective and non-reflective sections.

We evaluated the fabricated displacement sensor by capturing output signals from the sensor head, mounted on a precision stage, when the code scale is motor-driven in either the clockwise or counter-clockwise direction. Fig. 4(a) and (b) reveal the monitored quadrature pulse signals of Sig-A and B at a frequency of $\sim$130 kHz for the clockwise and counter-clockwise displacements, respectively. In the case of the clockwise displacement, Sig-A is witnessed to lead Sig-B, so as to exhibit a phase difference of positive 90°, whereas Sig-A lags behind Sig-B for the counter-clockwise case, resulting in the opposite phase relationship of negative 90°. Based on either Sig-A or Sig-B, we could secure a positional resolution of 10 μm and an angular resolution of $\sim$0.04°. When we utilize the quadrature phase relationship between the two signals, the positional and angular resolutions could be effectively upgraded to 2.5 μm and 0.01°, respectively, while the direction of displacement is efficiently discerned.

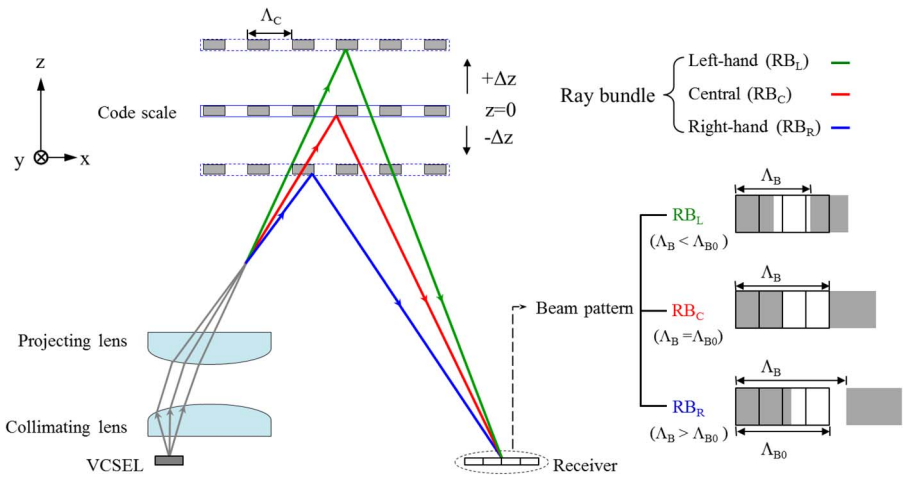

Fig. 5. Operation of the sensor capitalizing on a projected beam, depending on the vertical misalignment of the code scale.

4. Investigation Into the Structural Tolerance of the Proposed Displacement Sensor

We elaborated on the mechanism that underlies the structural tolerance of the proposed displacement sensor by focusing on the ray-optic properties of the projected beam. The variations in the beam pitch have been mainly verified by deliberately destroying the alignment of the major constituent elements in the horizontal/vertical direction, including the VCSEL, collimating lens, projecting lens, and code scale. We attempted to investigate the operation of the displacement sensor with respect to the structural tolerance by first taking the vertical misalignment of the code scale as an example. As depicted in Fig. 5, the projected beam is incident upon the code scale past the focal point. The beam is thought to consist of three representative bundles of rays: the central ray bundle (RB_C) in the middle, the left-hand (RB_L) and the right-hand ray bundle (RB_R). The projected beam is formed slightly inclined to the right, and the central bundle appears to be larger relative to the left-hand bundle and smaller relative to the right-hand bundle, in terms of the angle of propagation with respect to the z-axis. Originally, with the code scale positioned as designed, RB_C is deemed to reflect off the code scale so as to travel down to the PD-based receiver. When the code scale was misplaced upward by $+\Delta z$, RB_L instead of RB_C comes into play. On the other hand, when the code scale was misplaced downward by $-\Delta z$, RB_R plays a role in delivering sensing information. Since the three representative bundles have different angles of propagation, the pitch of the projected beam as measured at the site of the receiver changes according to the alignment of the code scale. According to the design, the reference value of the pitch of the projected beam is $\Lambda_{B0} = 160\ \mu$m at the receiver, as obtained in the case of the central ray bundle. The pitch Λ_B is anticipated to increase and decrease for the downward and upward misalignment with reference to the initial value, respectively. For the rest of the constituent elements, the pitch of the projected beam is also influenced by the alignment in a similar way. Specifically, the beam pitch is expected to increase as the VCSEL and the collimating lens deviate along the horizontal $+$x and $-$x axis, respectively, or when the projecting lens shifts to the upward $+$z direction. The pitch diminishes for the misalignment that occurs in the opposite directions, because the different portion of the projected beam will be mediated by the code scale, subject to the misalignment of the components. In accordance with the geometrical positions of the constituent components, the performance of the proposed sensor is consequently affected in terms of the phase relationship between its quadrature signals of Sig-A and Sig-B.

We then aimed to thoroughly probe into the structural tolerance of the passively assembled displacement sensor that resorts to the projected beam. The performance of the sensor is deemed to crucially rely on the pattern pitch of the projected beam traveling toward the receiver,

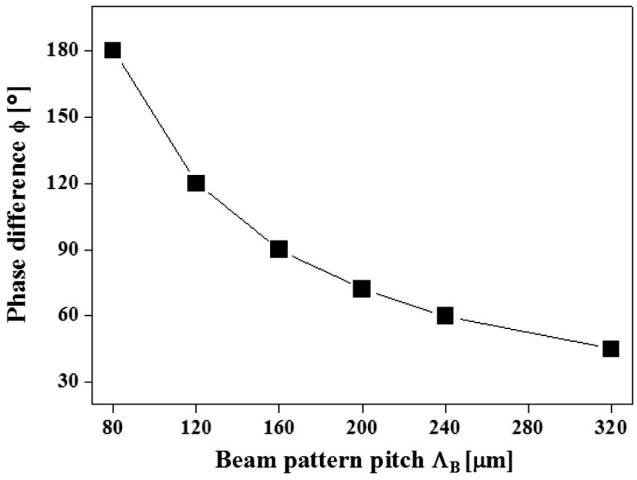

Fig. 6. Phase difference between the two output signals from the sensor in terms of the pattern pitch of the projected beam.

which is largely sensitive to the alignment among the constituent elements pertaining to the sensor. The positional tolerance that is relevant to the VCSEL, collimating/projecting lenses, and code scale is our primary concern, as mentioned above. We judged the pitch of the projected beam to be acceptable based on the condition that the sensor is capable of producing a pair of decent quadrature signals that represent a certain phase difference ϕ, which can then be applied to discern the direction of displacement and can provide a resolution that mimics the pitch of the code scale. In light of guaranteeing the discernment of the direction of displacement, we have merely permitted ϕ to deviate from a target value of 90° within $+/-$ 45°, i.e., from $\phi = 45°$ to 135°. The phase relationship between the two output signals in terms of the pattern pitch is plotted in Fig. 6. For the original case where $\Lambda_B = \Lambda_{B0} = 160$ μm, each of the four PD cells is supposed to admit one quarter of the pitch of the incoming beam. Therefore, the phase that is covered by a single PD tends to decline and rise with an increase and decrease in pitch, respectively. Specifically, the phase relationship is estimated to change from $\phi = 135°$ to 45°, with the pitch varying from 105 to 320 μm.

Considering that the propagation characteristics of the projected beam, particularly the pattern pitch, are primarily subject to the alignment of elements that comprise the displacement sensor, we simulated the influence of the horizontal misalignment of the VCSEL source and the collimating lens upon the pitch Λ_B, which is chiefly responsible for the projection point relative to the code scale. As plotted in Fig. 7(a), when the VCSEL shifted relative to the target position along the x-direction by an amount ranging from -100 to $+100$ μm, the pitch was altered from 128 to 208 μm. Similarly, the pitch changed from 208 to 124 μm, when the collimating lens was deviated along the direction of the x-axis from -100 to $+100$ μm. The results indicate that, within an acceptable variation in the phase difference between the two sensor signals ($+/-$ 45° with respect to 90°), which corresponds to Λ_B ranging from 105 to 320 μm, the maximum positional tolerances for the VCSEL and collimating lens were observed to be as large as $+/-$ 100 μm along the horizontal direction. As shown in Fig. 7(b), we then inspected the dependence of the pitch Λ_B upon the alignment of the projecting lens and the code scale. When the projecting lens was misaligned from the target position along the z-direction by a distance ranging from -100 to $+100$ μm, the pitch was altered from 132 to 196 μm. Similarly, the pitch changed from 196 to 136 μm when we position the code scale along the z-direction by a distance ranging from -100 to $+100$ μm. The maximum positional tolerances for the projecting lens and code scale were verified to be nearly $+/-$ 100 μm along the vertical direction, for an allowable range of Λ_B that incurs the same fluctuations in mutual phase relation (from $\phi = 45°$ to 135°). However, it should be remarked that the positional tolerance might be degraded to a certain extent if a tighter

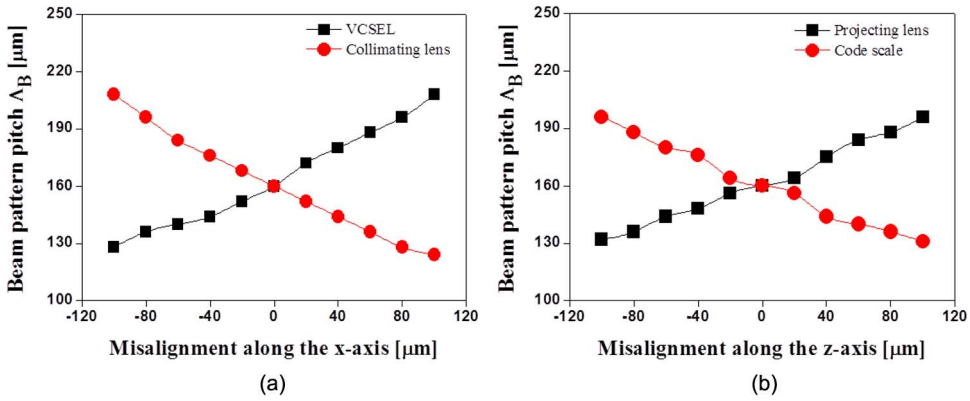

Fig. 7. Positional tolerance of the displacement sensor with respect to (a) the VCSEL source and the collimating lens and (b) the projecting lens and the code scale.

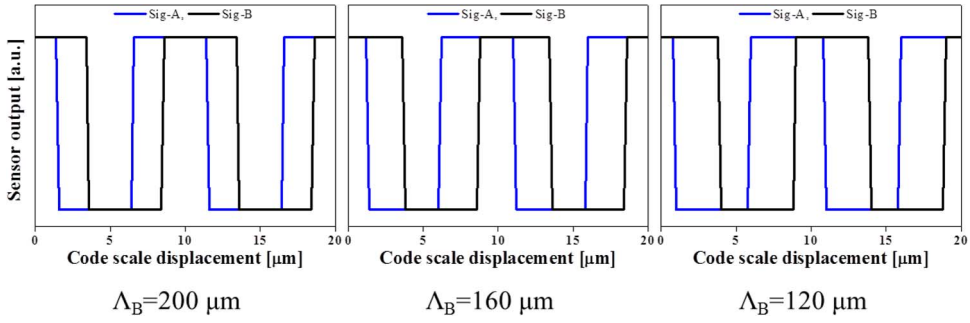

Fig. 8. Two output signals from the displacement sensor for various pitches of $\Lambda_B = 120$, 160, and 200 μm.

restriction is imposed upon the allowable variation in ϕ. The results presented in Fig. 7(a) and (b) therefore indicate that for the horizontal alignment along the x axis, the rate of change in the beam pattern pitch was nearly $+0.4$ μm/μm and -0.4 μm/μm for the VCSEL and the collimating lens, respectively. For the vertical alignment along the z axis, it was approximately $+0.3$ μm/μm and -0.36 μm/μm for the projecting lens and the code scale, respectively. Under a structural tolerance ranging to up to 100 μm, the sensor device was predicted to function normally, supplying a pair of well-defined quadrature signals.

Finally, we estimated the influence of the pitch of the projected beam upon the sensor output, due to the fact that the pitch should be definitely susceptible to the alignment of the constituent elements. Fig. 8 presents a pair of quadrature output signals for the different pitches of the traveling beam, with a fixed direction for the displacement, where we obtain $\phi = 72°$, 90°, and 120°, in response to $\Lambda_B = 200$, 160, and 120 μm, respectively. This signifies that, in spite of the variations in the beam pitch, the proposed sensor was able to practically distinguish the direction of the displacement, providing a positional resolution of 10 μm, which is equivalent to the pitch of the code scale. As a consequence of the theoretical analysis presented above, the proposed displacement sensor is believed to be highly tolerant in terms of the position of its constituent elements.

5. Conclusion

We presented a compact optical displacement sensor based on a projected beam, featuring a high structural tolerance. The grating pattern of the code scale encrypts the projected beam, which then conveys the displacement to an optical receiver consisting of four of PD cells connected in series. The magnitude and the direction of the displacement induced by the code

scale were accurately measured, by capitalizing on a pair of quadrature pulse signals resulting from the sensor. By rigorously exploring the influence of the positional errors of the major constituent components upon the pitch of the propagating projected beam, we proved that the passively constructed optical sensor leads to a highly relaxed structural tolerance, as anticipated, under the condition that the positional resolution is comparable to the pitch of the grating, and the direction of the displacement is clearly identified.

References

[1] H. Miyajima, E. Yamamoto, and K. Yanagisawa, "Optical micro encoder with sub-micron resolution using a VCSEL," *Sens. Actuators A, Phys.*, vol. 71, no. 3, pp. 213–218, Dec. 1998.

[2] A. Yacoot and N. Cross, "Measurement of picometre non-linearity in an optical grating encoder using X-ray interferometry," *Meas. Sci. Technol.*, vol. 14, no. 1, pp. 148–152, Jan. 2003.

[3] S. Makinouchi, A. Watanabe, M. Takasaki, T. Ohara, and J. Ong, "An evaluation of a modulated laser encoder," *Precis. Eng.*, vol. 35, no. 2, pp. 302–308, Apr. 2011.

[4] H. S. Lee and S. S. Lee, "Reflective optical encoder capitalizing on an index grating imbedded in a compact smart frame," *IEEE Photon. J.*, vol. 6, no. 2, 2014, Art. ID. 6800908.

[5] H. S. Lee and S. S. Lee, "Reflective-type photonics displacement sensor incorporating a micro-optic beam shaper," *Opt. Exp.*, vol. 22, no. 1, pp. 859–868, Jan. 2014.

[6] D. Crespo, J. Alonso, and E. Bernabeu, "Reflection optical encoders as three-grating moire systems," *Appl. Opt.*, vol. 39, no. 22, pp. 3806–3813, Aug. 2000.

[7] H. Miyajima *et al.*, "Optical micro encoder using a vertical-cavity surface-emitting laser," *Sens. Actuators A, Phys.*, vol. 57, no. 2, pp. 127–135, 1996.

[8] S. Wekhande and V. Agarwal, "High-resolution absolute position Vernier shaft encoder suitable for high-performance PMSM servo drives," *IEEE Trans. Instrum. Meas.*, vol. 55, no. 1, pp. 357–364, Feb. 2006.

[9] C. K. Lim, Z. Luo, I. Chen, and S. H. Yeo, "Wearable wireless sensing system for capturing human arm motion," *Sens. Actuators A, Phys.*, vol. 166, no. 1, pp.125–132, Mar. 2011.

[10] J. R. R. Mayer, "High-resolution of rotary encoder analog quadrature signals," *IEEE Trans. Instrum. Meas.*, vol. 43, no. 3, pp. 494–498, Jun. 1994.

[11] K. Hane, T. Endo, Y. Ito, and M. Sasaki, "A compact optical encoder with micromachined photodetector," *J. Opt. A, Pure Appl. Opt.*, vol. 3, no. 3, pp. 191–195, May 2001.

[12] J. Akedo, H. Machida, H. Kobayashi, Y. Shirai, and H. Ema, "Point source diffraction and its use in an encoder," *Appl. Opt.*, vol. 27, no. 22, pp. 4777–4781, Nov. 1988.

[13] C. F. Kao, H. L. Huang, and S. H. Lu, "Optical encoder based on fractional-Talbot effect using two-dimensional phase grating," *Opt. Commun.*, vol. 283, no. 9, pp. 1950–1955, May 2010.

[14] A. Lutenberg and F. Perez-Quintián, "Optical encoder based on a nondiffractive beam III," *Appl. Opt.*, vol. 48, no. 27, pp. 5015–5024, Sep. 2009.

[15] L. Liang *et al.*, "The design of composite optical encoder," in *Proc. 9th Int. Conf. Electron. Meas. Instrum.*, 2009, pp. 642–645.

[16] P. Aubert, H. J. Oguey, and R. Vuilleumier, "Monolithic optical position encoder with on-chip photodiodes," *IEEE J. Solid-State Circuits*, vol. 23, no. 2, pp. 465–473, Apr. 1988.

[17] K. Engelhardt and P. Seitz, "High-resolution optical position encoder with large mounting tolerances," *Appl. Opt.*, vol. 36, no. 13, pp. 2912–2916, May 1997.